# Macroscopic quantum states, quantum phase transition for $N$ three-level atoms in an optical cavity —— Gauge principle and non-Hermitian Hamiltonian

Ni Liu,[*] Xinyu Jia, and J.-Q. Liang[†]

We study in this paper the quantum phase transition (QPT) from normal phase (NP) to superradiant phase (SP) for $N$ three-level atoms in a single-mode optical cavity for both Hermitian and non-Hermitian Hamiltonians, where the $\Xi$-type three-level atom is described by spin-1 pseudo-spin operators. The long standing gauge-choice ambiguity of $\mathbf{A} \cdot \mathbf{p}$ and $\mathbf{d} \cdot \mathbf{E}$ called respectively the Coulomb and dipole gauges is resolved by the time-dependent gauge transformation on the Schrödinger equation. Both $\mathbf{A} \cdot \mathbf{p}$ and $\mathbf{d} \cdot \mathbf{E}$ interactions are included in the unified gauge, which is truly gauge equivalent to the minimum coupling principle. The Coulomb and dipole interactions are just the special cases of unified gauge. Remarkably three interactions lead to the same results under the resonant condition of field-atom frequencies, while significant difference appears in red and blue detunings. The QPT is analyzed in terms of spin-coherent-state variational method, which indicates the abrupt changes of energy spectrum, average photon number as well as the atomic population at the critical point of interaction constant. Crucially, we reveal the sensitive dependence on the initial optical-phase, which is particularly useful to test the validity of three gauges experimentally. The non-Hermitian atom-field interaction results in the exceptional point (EP), beyond which the semiclassical energy function becomes complex. However the energy spectrum of variational ground state is real in the absence of EP, and does not become complex. The superradiant state is unstable due to the non-Hermitian interaction induced photon-number loss. Thus only the NP exists in the non-Hermitian Dicke Model Hamiltonian.

## I. INTRODUCTION

Following the development of quantum computers [3, 46, 82, 83], the quantum manipulations based on cavity quantum electrodynamics grow incredibly fast [66] in the ultrastrong-coupling regime. As a result the field-atom coupling coefficient is comparable with the atom frequency, so that the quantum phase transition (QPT) becomes realistic in experiments [7, 54]. The ultrastrong or even superstrong coupling regimes have been realized experimentally in superconducting circuits [54, 73, 79] and various other platforms [28].

The QPT from normal phase (NP) to superradiant phase (SP) in Dicke model (DM), which describes $N$ identical two-level atoms in a single-mode optical cavity, has been extensively investigated theoretically and experimentally [2, 8, 20, 28, 30, 34, 39, 61, 63, 75, 81]. Multilevel atomic models, which are closer to realistic atomic structures, have attracted significant attention [56, 57] in recent years. The energy spectra of three-level atoms have been studied for $\Lambda-$ [59], $V-$ [26], and $\Xi-$type [25] of level configurations. The three-level configuration of atoms is related to an important class of quantum phenomena, including electromagnetically induced transparency [9, 27], lasing without inversion [50, 62], and quantum batteries [22, 23, 60] as well.

The extension from the two-level to three-level DM naturally provides a new perspective of atom-photon interactions[70]. The three-level DM exhibits rich physics, including subradiance [13, 15, 16, 78], SP transitions [5, 14, 31, 32], time crystals [35, 64], and chiral molecule detection[11].

The electron-photon interaction seems formally dependent on the gauge choice [4], which remains a long standing ambiguity, since measurable results must be gauge independent. Gauge invariance is a general requirement for the fundamental interactions [1, 47] in modern quantum field theory [1, 47, 76, 77]. Although the Hamiltonian of minimal coupling is gauge invariant, the approximate Hamiltonians may lead to different predictions for the light-matter interaction derived in different gauges [29, 33, 36, 37, 65]. Moreover, the convergence of the two-photon transition rate depends on the choice of the gauge significantly [6]. The gauge principle is violated by the quantum Rabi model with the dipolar coupling between a two-level atom and a quantized electromagnetic field [17, 18, 67]. This model has been used to describe various quantum systems and physical processes under different interaction regimes [28, 38]. The predictions based on the Rabi model drastically depend on the chosen gauge in the ultrastrong coupling regime. This gauge dependence is also an attribute in the finite-level truncation of the matter system.

The gauge ambiguities, which result from two fundamentally equivalent Hamiltonians, namely the minimal coupling and electric dipole Hamiltonians [58] respectively with $\mathbf{A} \cdot \mathbf{p}$ and $\mathbf{d} \cdot \mathbf{E}$ interactions [19, 43]. In the Rabi Hamiltonian, which is derived [68] from the minimal coupling, it is demonstrated that the failure of gauge invariance comes from the improper two-level truncation of the atomic Hilbert space [49]. The gauge ambiguities have been resolved recently [71] with a proper way of applying two-level truncation, from which the gauge-

invariant Rabi Hamiltonian is obtained.

We resolve the gauge ambiguity in this work from an alternative viewpoint. Since the Hamiltonian is explicitly time dependent. The time-dependent gauge transformation has to be applied on the time-dependent Schrődinger equation. The gauge equivalent Rabi Hamiltonian to the minimum coupling includes both the $\mathbf{A} \cdot \mathbf{p}$ and $\mathbf{d} \cdot \mathbf{E}$ interactions, which we called the unified gauge. The QPT for $N$ three-level atoms in a single-mode optical cavity is analyzed in term of the spin-coherent-state (SCS) variational method [39, 45, 75, 81] respectively in Coulomb, dipole and unified gauges as comparison. The novel phase effect of the optical field is incorporated in the energy function of unified gauge Hamiltonian, which reduces to the Coulomb and dipole gauges in the special phase value.

Non-Hermitian light-matter interactions have attracted considerable attention in both the semiclassical regime [24, 48, 72] and the quantum regime [21, 42, 69, 74], owing to their relevance to realistic physical scenarios of experiments [80]. Unconventional features of the SP transition have been revealed by incorporating non-Hermitian effects such as non-reciprocal couplings[12] or complex potentials[41, 44] into the DM. In the cavity dynamic system the non-Hermitian Hamiltonian exists naturally since the dipole matrix element $x_{ij}$ is a complex number with equal order of the real and imaginary parts [55]. The real value of $x_{ij}$ results in the non-Hermitian atom-field interaction. An exceptional point (EP) indeed emerges in the semiclassical energy function. However, the energy spectrum of variational ground state is real, with no complex value.

## II.  HAMILTONIAN OF THREE-LEVEL ATOM IN AN OPTICAL CAVITY AND THE GAUGE PRINCIPLE

The Hamiltonian for an electron in an atom can be written as

$$H_a = \frac{\mathbf{p}^2}{2m} + eV,$$

with three orthogonal eigenvectors denoted by $H_a|u_i\rangle = E_i|u_i\rangle$, where $i = 1, 2, 3$. The second-quantization Hamiltonian can be formally obtained in terms of the completeness projection operator

$$\widehat{P} = \sum_{i=1,2,3} |u_i\rangle \langle u_i|,$$

such as

$$\widehat{H}_a = \widehat{P} H_a \widehat{P} = \sum_{i=1,2,3} E_i|u_i\rangle \langle u_i|,$$

where the operator with hat denotes the second-quantization operator. According to the minimum coupling the Hamiltonian of electron in an optical cavity is

$$H(t) = \frac{[\mathbf{p} - e\mathbf{A}(t)]^2}{2m} + eV, \tag{1}$$

in the unit convention $c = \hbar = 1$ with $\mathbf{A}(t)$ being the time-dependent vector potential. The canonical momentum $\mathbf{p} = -i\nabla$ is as usual.

### A.  Coulomb gauge

The conventional Hamiltonian called Coulomb gauge with $\nabla \cdot \mathbf{A} = 0$ is derived as following

$$\widehat{H}(t) = \widehat{P} H \widehat{P} = \sum_{i=1,2,3} E_i|u_i\rangle \langle u_i| + \frac{\widehat{A}^2}{2m} + \widehat{H}_i, \tag{2}$$

in which the interaction part of Hamiltonian is

$$\widehat{H}_i(t) = -\sum_{i,j} |u_i\rangle \langle u_i| \frac{\widehat{A} \cdot \mathbf{p}}{m} |u_j\rangle \langle u_j|.$$

Using the relation

$$\frac{\mathbf{p}}{m} = \dot{\mathbf{x}} = i[H_a, \mathbf{x}] \tag{3}$$

the interaction part is obtained as

$$\widehat{H}_i(t) = i\widehat{A} \cdot \sum_{i \neq j} \mathbf{x}_{ij} (E_i - E_j) |u_i\rangle \langle u_j|, \tag{4}$$

where the quantized vector potential is

$$\widehat{A}(t) = \xi\mathbf{e} \left(\widehat{a}e^{-i\omega t} + \widehat{a}^\dagger e^{i\omega t}\right),$$

in the long-wave-length approximation with $\xi = \sqrt{\frac{1}{2\omega\epsilon_0}}$, and $\mathbf{e}$ being polarization unit vector. $\mathbf{x}_{ij} = \langle u_i|\mathbf{x}|u_j\rangle$ denotes the matrix elements of the electron position vector. We assume $\mathbf{x}_{12} = \mathbf{x}_{23}$, and $\mathbf{x}_{13} = 0$, which means that the cavity field does not generate the transition between levels 1 and 3. The dipole matrix element $\mathbf{x}_{12}$ is usually a complex number [55] with actually equal order of the real and imaginary parts [55]. The interaction Hamiltonian in Eq. (4) becomes

$$\begin{aligned}\widehat{H}_i(t) &= i\xi\mathbf{e}\left(\widehat{a}e^{-i\omega t} + \widehat{a}^\dagger e^{i\omega t}\right)\\&\quad \cdot[(E_3 - E_2)(\mathbf{x}_{32}|u_3\rangle\langle u_2| - \mathbf{x}_{23}|u_2\rangle\langle u_3|)\\&\quad + (E_2 - E_1)(\mathbf{x}_{21}|u_2\rangle\langle u_1| - \mathbf{x}_{12}|u_1\rangle\langle u_2|)].\end{aligned} \tag{5}$$

We adopt the dimensionless coupling constant $G = \xi\beta$ with

$$i\beta = \mathbf{e} \cdot \mathbf{x}_{12}, \quad -i\beta = \mathbf{e} \cdot \mathbf{x}_{21}, \tag{6}$$

in which the dipole matrix element $\mathbf{x}_{12}$ is regarded as the imaginary number in consistent with the $J - C$ model. For the equal level-space $\Xi$-type atom by setting $E_2 = 0, E_{3,1} = \pm\Omega$ respectively, the Hamiltonian becomes

$$\begin{aligned}\widehat{H}(t) &= \Omega\left(|u_3\rangle\langle u_3| - |u_1\rangle\langle u_1|\right)\\&\quad + G\Omega\left(\widehat{a}e^{-i\omega t} + \widehat{a}^\dagger e^{i\omega t}\right)\\&\quad \cdot\left(|u_3\rangle\langle u_2| + |u_2\rangle\langle u_1| + |u_2\rangle\langle u_3| + |u_1\rangle\langle u_2|\right),\end{aligned} \tag{7}$$

in which the quadratic field term $\frac{\widehat{A}^2}{2m}$ is neglected in the weak field approximation. The Hamiltonian can be represented in terms of spin$-1$ operator,

$$\widehat{H}_c = \Omega\widehat{s}_z + \frac{G\Omega}{\sqrt{2}}\left(\widehat{a}e^{-i\omega t} + \widehat{a}^\dagger e^{i\omega t}\right)\left(\widehat{s}_+ + \widehat{s}_-\right), \qquad (8)$$

with

$$\begin{aligned}\widehat{s}_z &= [|u_3\rangle\langle u_3| - |u_1\rangle\langle u_1|],\\ \widehat{s}_+ &= \sqrt{2}\left(|u_3\rangle\langle u_2| + |u_2\rangle\langle u_1|\right), \quad \widehat{s}_- = \widehat{s}_+^\dagger,\end{aligned}$$

It is easy to check that the spin commutation relations are satisfied,

$$[\widehat{s}_z, \widehat{s}_\pm] = \pm\widehat{s}_\pm, \quad [\widehat{s}_+, \widehat{s}_-] = 2\widehat{s}_z,$$

and

$$[\widehat{s}_x, \widehat{s}_y] = i\widehat{s}_z,$$

with

$$\widehat{s}_x = \frac{\widehat{s}_+ + \widehat{s}_-}{2}, \quad \widehat{s}_y = \frac{\widehat{s}_+ - \widehat{s}_-}{2i}.$$

We apply the time-dependent gauge transformation $|\psi'\rangle = \widehat{U}(t)|\psi\rangle$

$$i\frac{\partial}{\partial t}|\psi'\rangle = \widehat{H}'|\psi'\rangle, \qquad (9)$$

where

$$\widehat{H}' = \widehat{U}\widehat{H}\widehat{U}^\dagger - i\widehat{U}\frac{\partial}{\partial t}\widehat{U}^\dagger. \qquad (10)$$

Using unitary transformation operator

$$\widehat{U} = e^{-i\omega t\widehat{a}^\dagger\widehat{a}}, \qquad (11)$$

the final Hamiltonian of Coulomb gauge is time-independent

$$\widehat{H}_c = \widehat{H}' = \widehat{H}_0 + \widehat{H}_i^c, \qquad (12)$$

where

$$\widehat{H}_0 = \omega\widehat{a}^\dagger\widehat{a} + \Omega\widehat{s}_z \qquad (13)$$

and

$$\widehat{H}_i^c = \frac{G\Omega}{\sqrt{2}}\left(\widehat{a} + \widehat{a}^\dagger\right)\left(\widehat{s}_+ + \widehat{s}_-\right), \qquad (14)$$

is the Coulomb gauge interaction.

## B. *Dipole gauge*

The time-dependent vector potential generates an electric field

$$\mathbf{E} = -\frac{\partial\mathbf{A}}{\partial t},$$

and thus the Hamiltonian has an electric dipole interaction

$$H_d = H_a + H_i^d,$$

where

$$H_i^d = e\mathbf{x}\cdot\frac{\partial\mathbf{A}}{\partial t}. \qquad (15)$$

The Hamiltonian of second quantization is

$$\begin{aligned}\widehat{H}_i^d(t) &= \widehat{P}H_i^d\widehat{P} = G\omega\left(\widehat{a}e^{-i\omega t} - \widehat{a}^\dagger e^{i\omega t}\right)\\ &\cdot\left(|u_3\rangle\langle u_2| + |u_2\rangle\langle u_1| - c.c\right),\end{aligned} \qquad (16)$$

in which we assume that $\mathbf{e}\cdot\mathbf{x}_{ii} = 0$ for $i = 1, 2, 3$ due to the parity symmetry of atom energy levels. Following the same procedure as in the Coulomb gauge the time-independent Hamiltonian of dipole gauge is

$$\widehat{H}_d = \widehat{H}_0 + \widehat{H}_i^d, \qquad (17)$$

with the dipole gauge interaction given by

$$\widehat{H}_i^d = \frac{G\omega}{\sqrt{2}}\left(\widehat{a} - \widehat{a}^\dagger\right)\left(\widehat{s}_+ - \widehat{s}_-\right), \qquad (18)$$

which is quantitatively different from that in Coulomb gauge Eq. (14). One is proportional to energy difference $\Omega$ of atom while the other is proportional to the cavity-field frequency $\omega$. This controversy has lasted for more than half a century

## C. *The ambiguity of gauge choice*

Since the gauge potential $\mathbf{A}(t)$ is time-dependent, the total electric field is

$$\mathbf{E} = -\bigtriangledown\mathbf{V} - \frac{\partial\mathbf{A}(t)}{\partial t}. \qquad (19)$$

The Coulomb gauge Hamiltonian Eq. (14) does not include the energy term of electric field, $-\frac{\partial\mathbf{A}(t)}{\partial t}$, generated by the time-dependent gauge potential. The failure comes from the misplacing the canonical momentum $\mathbf{p}$ by the kinetic momentum $m\dot{\mathbf{x}}$ in Eq. (3). This misplacement would be no problem for the time independent gauge field, while the dipole interaction is missing for the time-dependent case. The energy term $e\mathbf{A}\cdot\mathbf{p}$ does

not exist in the dipole gauge since the interaction Eq. (15) is not derived directly from the standard minimum coupling Hamiltonian Eq. (1). Two gauges are both incomplete description of the atom-field interaction. This controversy can be resolved by the time-dependent gauge transformation on the time-dependent Schrödinger equation.

## III. TIME-DEPENDENT GAUGE TRANSFORMATION AND THE HAMILTONIAN OF UNIFIED GAUGE

We apply a time-dependent gauge transformation on the Schrödinger equation with the minimum coupling Hamiltonian Eq. (1) such that

$$i\frac{\partial}{\partial t}|\psi'\rangle = H'|\psi'\rangle,$$

where the $U(1)$ gauge transformation operator is given by [47]

$$R\left(t\right) = e^{-ie\mathbf{x}\cdot\mathbf{A}(t)}, \tag{20}$$

with $|\psi'\rangle = R|\psi\rangle$. The Hamiltonian in the new gauge is

$$H' = R\left(t\right)HR^{\dagger}\left(t\right) - iR\frac{\partial}{\partial t}R^{\dagger},$$

which recovers the dipole gauge Hamiltonian exactly [47]

$$H' = H_a + e\mathbf{x}\cdot\frac{\partial\mathbf{A}\left(t\right)}{\partial t}.$$

If we would directly take the second quantization procedure with identity density operator $\widehat{I}$, the dipole gauge Hamiltonian should be obtained. Then the $\mathbf{A}\cdot\mathbf{p}$ interaction would be lost. We argue that the gauge equivalence includes not only the Hamiltonian but also the state vector. Since the Hamiltonian is in the new gauge with the state vector $|\psi'\rangle = R|\psi\rangle$, inserting the completeness operator we have

$$|\psi'\rangle = R\sum_{i=1,2,3}|u_i\rangle\langle u_i|\psi\rangle = \sum_{i=1,2,3}|u_i'\rangle\langle u_i|\psi\rangle = \widehat{P}'|\psi\rangle.$$

The identity density operator in the new gauge becomes $\widehat{P}'$ and thus the second quantization has to be applied with the transformed operator $\widehat{P}'$. The Hamiltonian of unified gauge is then derived such as

$$\begin{aligned}\widehat{H}_u &= \left(\widehat{P}'\right)^{\dagger}H'\widehat{P}' \\ &= \widehat{P}\left(H + ex\cdot\frac{\partial A(t)}{\partial t}\right)\widehat{P} \\ &= \widehat{H}_a + \widehat{H}_i^c(t) + \widehat{H}_i^d(t), \end{aligned} \tag{21}$$

in which the Hamiltonian $H$ in the second equality is given in Eq. (1) for the atom in the cavity field. The

Hamiltonian of second quantization contains two parts of interaction. The first one is exactly that of Coulomb gauge in Eq. (2), while the second part is the interaction Hamiltonian of dipole gauge given in Eq. (16). Following the same procedure of time-dependent gauge transformation Eqs. (9), (10) and (11) of the previous section we obtain the time-independent Hamiltonian of unified gauge

$$\widehat{H}_u = \widehat{H}_0 + \widehat{H}_i^c + \widehat{H}_i^d, \tag{22}$$

in which $\widehat{H}_0$, $\widehat{H}_i^c$, and $\widehat{H}_i^d$ are given respectively in Eqs. (13), (14) and (18). The Hamiltonian Eq. (22) is truly gauge equivalent to the minimum coupling one Eq. (1).

## IV. DM HAMILTONIAN OF THREE-LEVEL ATOMS, MACROSCOPIC QUANTUM STATES AND QPT

For $N$ identical three-level atoms, we have the constraint

$$\sum_{l=1}^{N}\widehat{P}_l = N\widehat{P}.$$


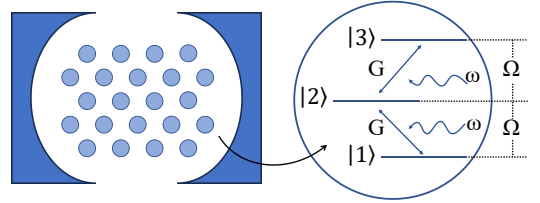
FIG. 1: Diagram of the extended DM with N three-level atoms in an optical cavity. Atomic states$|1\rangle$(bottom), $|2\rangle$(middle), and $|3\rangle$(top) are shown by black horizontal bars. Curved arrows denote photons of frequency $\omega$, while solid arrows indicate light-matter interactions between atomic and cavity modes, with dimensionless coupling constant G between the light field and atoms

Our theoretical model, schematically depicted in Fig. 1, comprises N $\Xi$-type three-level atoms coupled to an optical cavity.

The spin-operator Hamiltonian Eq. (14) with spin value 1 is extended to high spin value $s$. It is crucial to establish the relation between atom number $N$ and spin value $s$.The number of eigenstates for spin-$s$ is $2s+1$.For $N$ identical atoms distributed in three levels there exist $2N+1$ eigenstates. Thus, we have $s = N$ different from the two-level case, where $s = N/2$. The DM Hamiltonian for three-level atoms is simply replaced by spin-$s$ operators

$$\widehat{H}_u = \omega\widehat{a}^\dagger\widehat{a} + \Omega\widehat{S}_z + \frac{G\Omega}{\sqrt{2N}}\left(\widehat{a} + \widehat{a}^\dagger\right)\left(\widehat{S}_+ + \widehat{S}_-\right)$$
$$+ \frac{G\omega}{\sqrt{2N}}\left(\widehat{a} - \widehat{a}^\dagger\right)\left(\widehat{S}_+ - \widehat{S}_-\right), \quad (23)$$

where $\widehat{S}_z$ and $\widehat{S}_\pm$ now are collective, atomic spin operators.

### A. SCS variational method, macroscopic quantum states and QPT

We are going to demonstrate the macroscopic quantum states and QPT in terms of SCS variational method [39, 45, 75, 81], which is valid for arbitrary number of atoms $N$. To this end we begin with the average of Hamiltonian in the optical coherent state $|\alpha\rangle$, which is assumed as the boson coherent state of cavity mode such that $a|\alpha\rangle = \alpha|\alpha\rangle$, where the complex eigenvalue is parametrized as

$$\alpha = \gamma e^{i\varphi}. \quad (24)$$

After the average in the boson coherent state we obtain an effective Hamiltonian of the pseudo-spin operators

$$\widehat{H}_{eff}(\alpha) = \langle\alpha|\widehat{H}|\alpha\rangle. \quad (25)$$

The effective spin Hamiltonian can be diagonalized in the SCSs of north- and south-pole gauges [39, 45, 75, 81] defined by

$$\widehat{R}|\pm u\rangle = |s, \pm s\rangle \quad (26)$$

$$\widehat{R} = e^{-\frac{\theta}{2}\left(\widehat{S}_+ e^{-i\varphi} - \widehat{S}_- e^{i\varphi}\right)}, \quad (27)$$

where $\theta$ is a pending parameter to be determined. Through a unitary transformation via the unitary operator $\widehat{R}$, the spin operators $\widehat{S}_z, \widehat{S}_+, \widehat{S}_-$ transform as follows:

$$\widehat{R}\widehat{S}_z\widehat{R}^\dagger = \widehat{S}_z\cos\theta + \frac{1}{2}\left(e^{-i\varphi}\widehat{S}_+\sin\theta + e^{i\varphi}\widehat{S}_-\sin\theta\right)$$
$$\widehat{R}\widehat{S}_+\widehat{R}^\dagger = \widehat{S}_+\cos^2\frac{\theta}{2} - e^{i\varphi}\widehat{S}_z\sin\theta - \widehat{S}_- e^{2i\varphi}\sin^2\frac{\theta}{2}$$
$$\widehat{R}\widehat{S}_-\widehat{R}^\dagger = \widehat{S}_-\cos^2\frac{\theta}{2} - e^{-i\varphi}\widehat{S}_z\sin\theta - \widehat{S}_+ e^{-2i\varphi}\sin^2\frac{\theta}{2}.$$

We in the followings are going to find the energy spectrum of the SCS by means of the variational method with respect to the variation parameter $\gamma$ respectively for three-type of gauge as a comparison.

### B. Coulomb gauge

The effective spin Hamiltonian of Coulomb gauge is found after the unitary transformation as

$$\widehat{R}\widehat{H}_{eff}^c\widehat{R}^\dagger = \omega\gamma^2 + A\widehat{S}_z + B\widehat{S}_+ + \widehat{C}\widehat{S}_-, \quad (28)$$

in which

$$A = \Omega\cos\theta - \frac{2\sqrt{2}}{\sqrt{N}}G\Omega\gamma\cos^2\varphi\sin\theta,$$
$$B = \frac{\Omega e^{-i\varphi}}{2}\sin\theta + \frac{\sqrt{2}G\Omega}{\sqrt{N}}\gamma\cos\varphi(\cos^2\frac{\theta}{2} - e^{-2i\varphi}\sin^2\frac{\theta}{2}),$$
$$C = \frac{\Omega e^{i\varphi}}{2}\sin\theta + \frac{\sqrt{2}G\Omega}{\sqrt{N}}\gamma\cos\varphi(\cos^2\frac{\theta}{2} - e^{2i\varphi}\sin^2\frac{\theta}{2}).$$

The effective spin Hamiltonian Eq. (28) can be diagonalized with the SCS Eq. (26) under the condition $B = 0$ and $C = 0$, which give rise to $\varphi = 2n\pi$. And the pending parameter is found as

$$\cos\theta = \pm\frac{1}{\sqrt{1 + 2^3\frac{G^2}{N}\gamma^2}}.$$

We obtain the semiclassical energy functions in the SCS corresponding respectively to the ground and highest excited-states

$$E_\pm^c(\gamma) = \langle\pm u|\widehat{H}_{eff}^c|\pm u\rangle = \omega\gamma^2 \pm N\Omega\sqrt{1 + \frac{2^3 G^2\gamma^2}{N}}.$$

The average energy function of per atom is

$$\varepsilon_\pm(\gamma) = \frac{E_\pm(\gamma)}{N} = \frac{\omega\gamma^2}{N} \pm \Omega\sqrt{1 + \frac{2^3\gamma^2 G^2}{N}}. \quad (29)$$

According to the variational method the energies of macroscopic quantum states are determined from the extremum condition of the energy function

$$\frac{\partial\varepsilon_\pm}{\partial\gamma} = \frac{2\gamma}{N}\left(\omega \pm \frac{2^2 G^2\Omega}{\sqrt{1 + \frac{2^3\gamma^2 G^2}{N}}}\right) = 0. \quad (30)$$

The extremum equation Eq. (30) always possesses a zero photon-number solution

$$\gamma = 0,$$

which is called the normal phase (NP) if the second-order derivative is positive

$$\frac{\partial^2\varepsilon_-}{\partial\gamma^2}(\gamma = 0) = \frac{2}{N}\left(\omega - 4G^2\Omega\right) \geq 0.$$

The phase boundary of NP is determined from the equal sign

$$G_c = \frac{1}{2}\sqrt{\eta}, \quad (31)$$

in which

$$\eta = \frac{\omega}{\Omega} \quad (32)$$

denotes the ration of field and atom frequencies. The NP with

$$\varepsilon_- = -\Omega$$

exists in the region

$$G \leq G_c.$$

The second-order derivative of the energy function for the spin-up $(\varepsilon_+)$ state is always positive

$$\frac{\partial^2 \varepsilon_+}{\partial \gamma^2}(\gamma = 0) > 0.$$

Thus the zero photon state $\varepsilon_+ = \Omega$ is stable in the entire region of coupling value.

The stable macroscopic state of nonzero photon number for energy function $\varepsilon_-$ is determined from the extremum condition Eq. (30). The nonzero solution is found as

$$\gamma_c = \frac{\sqrt{N}\sqrt{(4G^2\frac{1}{\eta})^2 - 1}}{2\sqrt{2}G}, \tag{33}$$

which is called the superradiant phase (SP) if the second-order derivative of the energy function is positive,

$$\frac{\partial^2 \varepsilon_-}{\partial \gamma^2}(\gamma_c) \geq 0.$$

The equal sign gives rise to exactly the same phase boundary $G_c$ in Eq. (31). The SP exists in the region $G > G_c$. The extremum equation Eq. (30) does not have a nonzero photon solution for the energy function $\varepsilon_+(\gamma)$.

The average photon number per atom, energy and atomic population imbalance between the two atom levels $\pm\Omega$ in SP are given respectively by

$$n_p = \frac{\gamma_c^2}{N} = \frac{(2^2G^2\frac{1}{\eta})^2 - 1}{2^3 G^2},$$

$$\varepsilon_- = \omega n_p - \Omega\sqrt{1 + 2^3 n_p G^2},$$

and

$$\Delta n_a = \frac{\langle -u|\,\widehat{S}_z\,|-u\rangle}{N} = -\frac{1}{\sqrt{1 + 2^3 n_p G^2}},$$

which are depicted in fig. 2 with respect to the dimensionless coupling constant $G$.

## C. Dipole gauge

The effective spin Hamiltonian of dipole gauge $\widehat{H}_{eff}^d$ has the same form of Eq. (28) after unitary transformation with

$$A = \Omega \cos\theta + \frac{2\sqrt{2}G}{\sqrt{N}}\gamma\omega \sin^2\varphi \sin\theta,$$



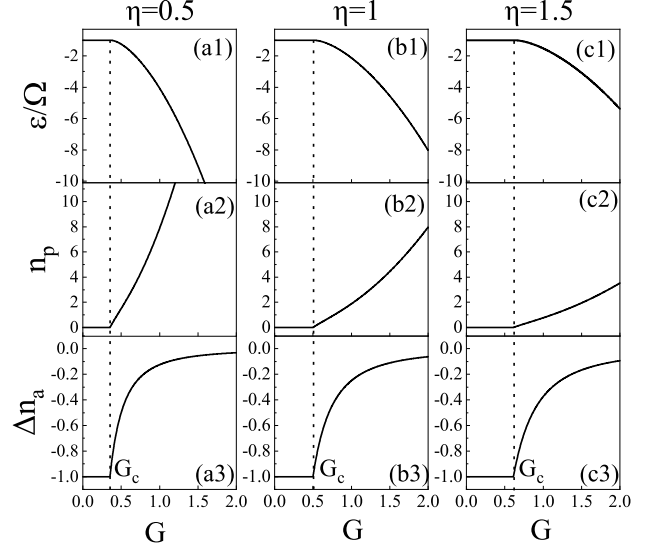FIG. 2: Energy spectrum $\varepsilon_-$ (1), photon number $n_p$ (2), and atomic population $n_a$ in the Coulomb gauge respectively for red detuning $\eta = 0.5$ (a), resonance $\eta = 1$ (b), blue detuning $\eta = 1.5$ (c). The phase transition point $G_c$ shifts to the higher value with the increase of detuning.

$$B = \frac{\Omega e^{-i\varphi}}{2}\sin\theta + i\frac{\sqrt{2}G\omega}{\sqrt{N}}\gamma\sin\varphi\left(\cos^2\frac{\theta}{2} + e^{-2i\varphi}\sin^2\frac{\theta}{2}\right),$$

$$C = \frac{\Omega e^{i\varphi}}{2}\sin\theta - i\frac{\sqrt{2}G\omega}{\sqrt{N}}\gamma\sin\varphi(e^{2i\varphi}\sin^2\frac{\theta}{2} + \cos^2\frac{\theta}{2}).$$

The pending parameter $\theta$ is determined under the condition $B = C = 0$,

$$\cos\theta = \pm\frac{1}{\sqrt{1 + 2^3 G^2\frac{\gamma^2}{N}\eta^2}}, \tag{34}$$

with the field phase given by $\varphi = \frac{\pi}{2} + 2n\pi$. Finally the average energy functions of per atom are found in the SCS $|\pm u>$ as

$$\varepsilon_\pm = \frac{\omega\gamma^2}{N} \pm \Omega\sqrt{1 + \frac{2^3\gamma^2 G^2\eta^2}{N}}.$$

The extremum equation

$$\frac{\partial \varepsilon_\pm}{\partial \gamma} = \frac{2\gamma\omega}{N}\left(1 \pm \frac{2^2 G^2\eta}{\sqrt{1 + \frac{2^3\gamma^2 G^2\eta^2}{N}}}\right) = 0 \tag{35}$$

always possesses a zero photon-number solution $\gamma = 0$.

The second-order derivative of the energy function for the spin-up state $(\varepsilon_+)$ is always positive

$$\frac{\partial^2 \varepsilon_+}{\partial \gamma^2}(\gamma = 0) = \frac{2\omega}{N}\left(1 + 2^2 G^2\eta\right) > 0,$$

which means that the macroscopic quantum state $\varepsilon_+$ is stable same as in the Coulomb gauge.

The nonzero photon solution for the spin-down state is obtained from the extremum equation

$$\frac{\partial \varepsilon_-}{\partial \gamma} = \frac{2\gamma\omega}{N}\left(1 - \frac{2^2 G^2 \eta}{\sqrt{1 + \frac{2^3 \gamma^2 G^2 \eta^2}{N}}}\right) = 0, \qquad (36)$$

which gives rise to the zero photon solution $\gamma = 0$ and the nonzero photon solution

$$\gamma_c = \frac{\sqrt{N}}{2\sqrt{2}}\sqrt{2^4 G^2 - \left(\frac{1}{G\eta}\right)^2}. \qquad (37)$$

The stable zero photon solution satisfies the condition

$$\frac{\partial^2 \varepsilon_-}{\partial \gamma^2}\left(\gamma = 0\right) = \frac{2\omega}{N}\left(1 - 2^2 G^2 \eta\right) \geq 0.$$

The NP exists in the region

$$G \leq G_c,$$

with the phase boundary given by

$$G_c = \frac{1}{2}\sqrt{\frac{1}{\eta}}, \qquad (38)$$

which is different from that of Coulomb gauge Eq.(31). The stable nonzero-photon state, namely the SP, is verified by the positive second-order derivative

$$\frac{\partial^2 \varepsilon_-}{\partial \gamma^2}\left(\gamma_c\right) \geq 0,$$

in which the equality results also in the phase boundary Eq.(38) between NP and the SP. The average photon number of per atom, energy and atomic population imbalance are given respectively by

$$n_p = \frac{\gamma_c^2}{N} = \frac{1}{2^3}\left[2^4 G^2 - \left(\frac{1}{G\eta}\right)^2\right], \qquad (39)$$

$$\varepsilon_- = \omega n_p \pm \Omega\sqrt{1 + 2^3 n_p G^2 \eta^2}, \qquad (40)$$

and

$$\Delta n_a = -\frac{1}{\sqrt{1 + 2^3 n_p G^2 \eta^2}},$$

which reduces to the well known result in the NP that $\Delta n_a = -1$.

Corresponding quantities ($\varepsilon_-$, $n_p$, $\Delta n_a$) in the dipole gauge are shown in Fig. 3. The phase transition point $G_c$ moves to the opposite direction with increase of the atom-field frequency detuning respectively in the Coulomb and dipole gauges, while has equal value $\frac{1}{2}$ in the resonance $\eta = 1$. Fig. 4 is the phase diagram in $G-\eta$ space for both gauges. Phase boundary separates the NP (dark purple region) and SP with the photon number $n_p$ in color scale. Critical observation is that the SP region decreases (increases) with the increasing detuning $\eta$ in Coulomb (dipole) gauge consistent with Figs. 2 and 3.
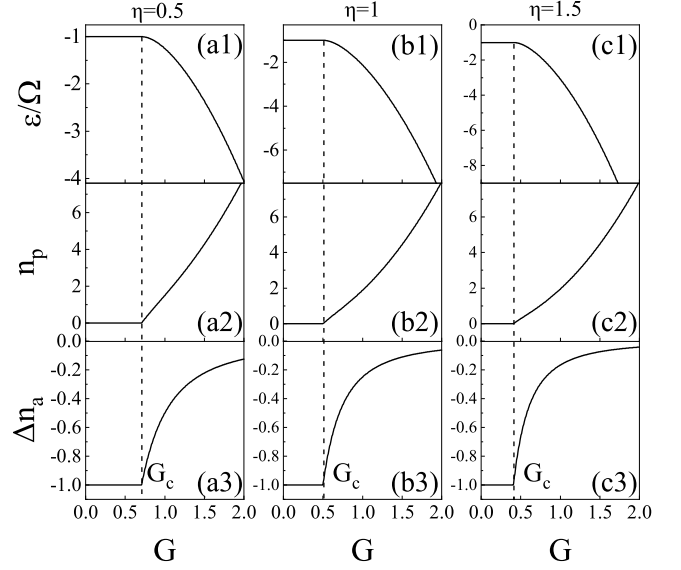


FIG. 3: The energy spectrum $\varepsilon_-$ (1), photon number $n_p$ (2) and atomic population $\Delta n_a$ (3) in the dipole gauge respectively for red-detuning (a), resonance (b), and blue-detuning (c). The phase transition point $G_c$ shifts to the lower value with the increase of detuning.
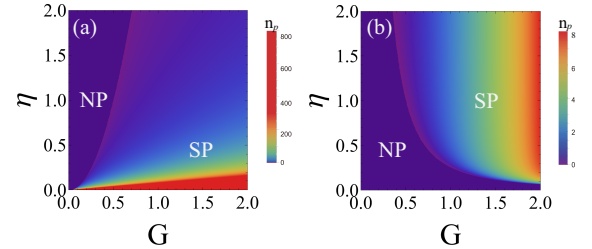


FIG. 4: Phase diagrams in $G-\eta$ space for Coulomb gauge (a) and dipole gauge (b). The photon number $n_p$ in SP is indicated by color scale.

### D. Unified gauge

For the effective spin Hamiltonian Eq. (25) in the unified gauge the unitary transformation operator Eq. (27) has to be modified as

$$\widehat{R} = e^{-\frac{\theta}{2}\left(\widehat{S}_+ e^{-i\phi} - \widehat{S}_- e^{i\phi}\right)},$$

in which $\theta$, $\phi$ are two pending parameters to be determined. After the unitary transformation the effective spin Hamiltonian has the same form of Eq. (28) with

$$B = G\sqrt{\frac{2}{N}}\gamma[\Omega\cos\varphi(\cos^2\frac{\theta}{2} - e^{-2i\phi}\sin^2\frac{\theta}{2}) + i\omega\sin\varphi(\cos^2\frac{\theta}{2} + e^{-2i\phi}\sin^2\frac{\theta}{2})] + \frac{1}{2}\Omega\sin\theta e^{-i\phi},$$

$$C = G\sqrt{\frac{2}{N}}\gamma[\Omega\cos\varphi(\cos^2\frac{\theta}{2} - e^{i2\phi}\sin^2\frac{\theta}{2})$$
$$-i\omega\sin\varphi(e^{i2\phi}\sin^2\frac{\theta}{2} + \cos^2\frac{\theta}{2})] + \frac{1}{2}\Omega\sin\theta e^{i\phi},$$

and

$$A = \Omega\cos\theta + \frac{2\sqrt{2}\gamma}{\sqrt{N}}G\sin\theta(\omega\sin\varphi\sin\phi - \Omega\cos\varphi\cos\phi).$$

The pending parameters $\phi$ and $\theta$ are determined by the condition $B = C = 0$ that

$$\cos\phi = \frac{\cos\varphi}{\sqrt{\Phi(\eta,\varphi)}},$$

in which

$$\Phi(\eta,\varphi) = \cos^2\varphi + \eta^2\sin^2\varphi,$$

is a function of cavity-field phase $\varphi$ in Eq.(24). We have

$$\cos\theta = \pm\frac{1}{\sqrt{1 + 2^3G^2\frac{\gamma^2}{N}\Phi(\eta,\varphi)}},$$

and

$$A = \Omega\sqrt{1 + 2^3G^2\frac{\gamma^2}{N}\Phi(\eta,\varphi)}. \quad (41)$$

The semiclassical energy function of per atom in the SCS $|\pm u>$ depends on the field phase $\varphi$

$$\varepsilon_\pm(\gamma,\varphi) = \omega\frac{\gamma^2}{N} \pm A, \quad (42)$$

which reduces to the energy functions of Coulomb and dipole gauges respectively in $\varphi = 0, \frac{\pi}{2}$. The extremum equation

$$\frac{\partial\varepsilon_\pm}{\partial\gamma} = 0 \quad (43)$$

possesses the zero photon solution $\gamma = 0$, which is stable for the spin down state $\varepsilon_-$ under the condition

$$\frac{\partial^2\varepsilon_-}{\partial\gamma^2}(\gamma = 0) \geq 0.$$

The boundary condition is found from the equality

$$G_c = \frac{1}{2}\sqrt{\frac{\eta}{\Phi(\eta,\varphi)}}, \quad (44)$$

which is the same value $G_c = \frac{1}{2}$ in the resonance $\eta = 1$ independent of the gauge choice. The spin down state with energy $\varepsilon_-$ is called the NP in the region $G < G_c$. The spin up state of $\varepsilon_+$ with population inversion is stable since the second derivative of energy function, $\frac{\partial^2\varepsilon_+}{\partial\gamma^2}(\gamma = 0) > 0$, is always greater than 0.

The nonzero photon solution of the extremum equation Eq. (39) for spin down state given by

$$\gamma_c = \sqrt{N}\sqrt{\frac{2G^2\Phi(\eta,\varphi)}{\eta^2} - \frac{1}{2^3G^2\Phi(\eta,\varphi)}}. \quad (45)$$

The stable ground state, namely the SP, is verified by the positive second-order derivative

$$\frac{\partial^2\varepsilon_-}{\partial\gamma^2}(\gamma_c) \geq 0,$$

in which the equality equation results also in the phase boundary Eq. (44) between NP and the SP. The average photon number of per atom, energy and atomic population imbalance for the SP are respectively given by

$$n_p = \frac{\gamma_c^2}{N}$$

$$\varepsilon_-(n_p) = \omega n_p - \Omega\sqrt{1 + 2^3G^2n_p\Phi(\eta,\varphi)} \quad (46)$$

and

$$\Delta n_a = -\frac{1}{\sqrt{1 + 2^3G^2n_p\Phi(\eta,\varphi)}}, \quad (47)$$

which reduce to those in Coulomb gauge for $\varphi = 0$ and dipole gauge for $\varphi = \pi/2$. These quantities are plotted in Fig. 5 respectively for field phases $\varphi = \pi/6, \pi/4, \pi/3$ indicating the phase-sensitive behavior. They are the same at resonance independent of the gauge and the phase angle $\varphi$. The increase of photon number with coupling $G$ slows slightly when phase angle $\varphi$ increases in the red detuning seen from Fig. 5 (b1). While the situation is just opposite in the blue detuning [Fig. 5 (b3)].

Fig. 6 presents $G - \eta$ phase diagrams in the unified gauge for different optical phases $\varphi = \pi/6, \pi/4, \pi/3$ indicating the continuos variation of the phase boundary and photon number in SP with respect to $G$ and $\eta$.

The geometric phase induced by the light field can be found by solving the Schrődinger equation with the time-dependent Hamiltonian Eq. (21).

Using the unitary transformation Eq. (20) the non-adiabatic Berry phase in the ground state $|\psi\rangle = |\alpha\rangle|-u\rangle$ is found as [10, 40]

$$\Gamma = i\int_0^T \langle\psi|\widehat{U}\frac{\partial}{\partial t}\widehat{U}^\dagger|\psi\rangle dt = 2\pi\langle\alpha|\widehat{a}^\dagger\widehat{a}|\alpha\rangle = 2\pi\gamma^2. \quad (48)$$

The average geometric phase of per atom is zero in NP and

$$\Upsilon = \frac{\Gamma}{N} = 2\pi n_p,$$

in the SP. It is well known that the Berry phase can characterize the QPT and the critical property at the phase transition point $G_c$.
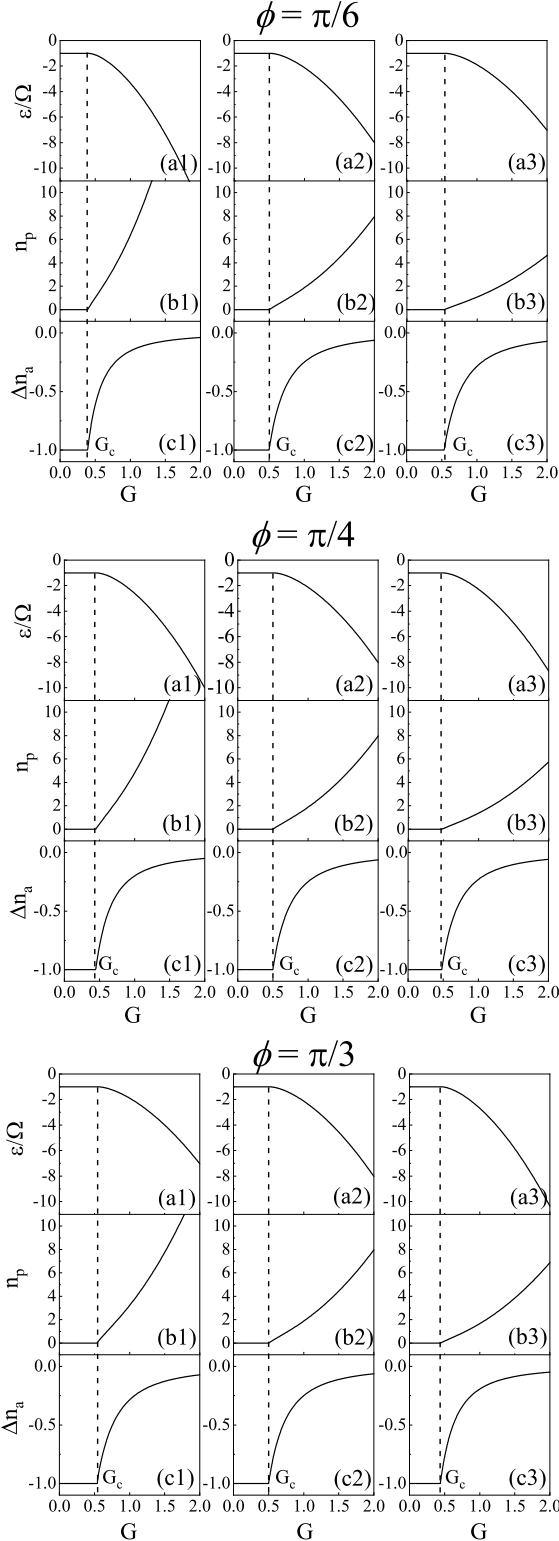
FIG. 5: The energy spectrum $\varepsilon_-$ (a), photon number $n_p$ (b) and atomic population $\Delta n_a$ (c) at fixed field phases $\phi = \pi/6, \pi/4, \pi/3$ for red detuning $\eta = 0.5$ (1), resonance $\eta = 1$ (2), blue detuning $\eta = 1.5$ (3).

## V. NON-HERMITIAN HAMILTONIAN, EXCEPTIONAL POINT AND GROUND STATE

The non-Hermitian Hamiltonian has become a hot topic in resent years. The interaction constant $G$ in the DM is proportional to dipole matrix element $\mathbf{x}_{ij}$, which is a complex number with equal order of real and imaginary parts [55]. The Hermitian interaction is obtained with the imaginary value of $\mathbf{x}_{ij}$. It is certainly interesting to see the phenomena of non-Hermitian cavity-atom coupling with the real part of the matrix element $\mathbf{x}_{ij}$ Eq. (6). The non-Hermitian Hamiltonian of DM can be expressed as

$$
\begin{aligned}
\widehat{H}_u &= \omega \widehat{a}^\dagger \widehat{a} + \Omega \widehat{S}_z + \frac{iG}{\sqrt{2N}}[\Omega \left(\widehat{a} + \widehat{a}^\dagger\right) \left(\widehat{S}_+ + \widehat{S}_-\right) \\
&\quad + \omega \left(\widehat{a} - \widehat{a}^\dagger\right) \left(\widehat{S}_+ - \widehat{S}_-\right)].
\end{aligned}
\tag{49}
$$

After the average in the boson coherent state we obtain an effective Hamiltonian of the pseudospin operators in the unified gauge

$$
\begin{aligned}
\widehat{H}_{eff} &= \omega \gamma^2 + \Omega \widehat{S}_z + \frac{\sqrt{2}G\gamma}{\sqrt{N}}[i\Omega \cos\varphi \left(\widehat{S}_+ + \widehat{S}_-\right) \\
&\quad - \omega \sin\varphi \left(\widehat{S}_+ - \widehat{S}_-\right)],
\end{aligned}
\tag{50}
$$

which is non-Hermitian

$$
\begin{aligned}
\widehat{H}_{eff}^\dagger &= \omega \gamma^2 + \Omega \widehat{S}_z + \frac{\sqrt{2}G\gamma}{\sqrt{N}}[-i\Omega \cos\varphi \left(\widehat{S}_+ + \widehat{S}_-\right) \\
&\quad + \omega \sin\varphi \left(\widehat{S}_+ - \widehat{S}_-\right)].
\end{aligned}
\tag{51}
$$

According to the theory of Mostafazadeh [51–53] the non-Hermitian Hamiltonian with real spectrum can be transformed to a Hermitian one by a similarity transformation. This is called the pseudo-symmetry, which in the present case is

$$
\widehat{R}\widehat{H}_{eff}\widehat{R}^{-1} = \widehat{h} = \widehat{h}^\dagger.
\tag{52}
$$

The Hermitian transformation operator is seen to be [45]

$$
\widehat{R} = e^{-\frac{\theta}{2}\left(\widehat{S}_+ e^{i\phi} + \widehat{S}_- e^{-i\phi}\right)}.
\tag{53}
$$

Using the transformation form

$$
\begin{aligned}
\widehat{R}\widehat{S}_z\widehat{R}^{-1} &= \widehat{S}_z \cosh\theta + \frac{1}{2}e^{i\phi}\widehat{S}_+ \sinh\theta - \frac{1}{2}e^{-i\phi}\widehat{S}_- \sinh\theta, \\
\widehat{R}\widehat{S}_+\widehat{R}^{-1} &= \widehat{S}_+ \cosh^2\frac{\theta}{2} + e^{-i\phi}\widehat{S}_z \sinh\theta - \widehat{S}_- e^{-2i\phi} \sinh^2\frac{\theta}{2}, \\
\widehat{R}\widehat{S}_-\widehat{R}^{-1} &= \widehat{S}_- \cosh^2\frac{\theta}{2} - e^{i\phi}\widehat{S}_z \sinh\theta - \widehat{S}_+ e^{2i\phi} \sinh^2\frac{\theta}{2}.
\end{aligned}
$$

The effective spin Hamiltonian $\widehat{H}_{eff}$ possesses the same form Eq. (28) with

$$
A = \Omega \cosh\theta + \frac{2\sqrt{2}G\gamma}{\sqrt{N}}(\Omega \cos\varphi \sin\phi - \omega \sin\varphi \cos\phi)\sinh\theta,
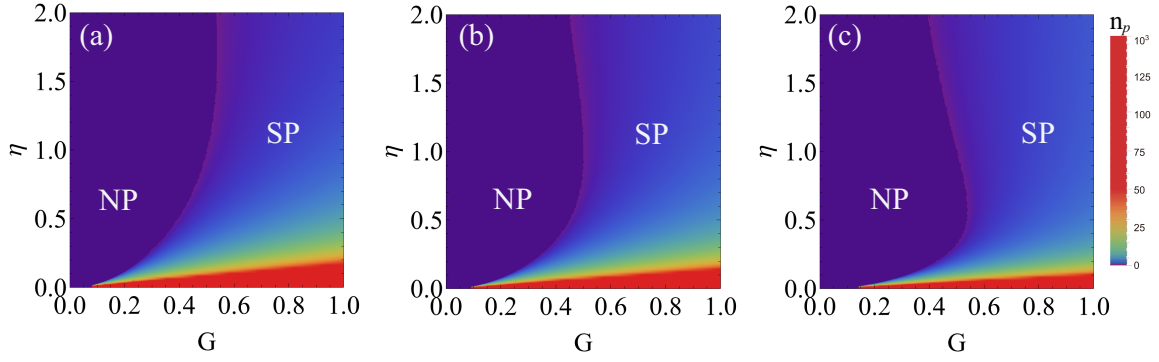$$

FIG. 6: Phase diagrams in $G - \eta$ space for cavity-field phases $\varphi = \pi/6$ (a), $\pi/4$ (b) , $\pi/3$ (c).

$$B = \frac{\sqrt{2}G\gamma}{\sqrt{N}}[i\Omega\cos\varphi(\cosh^2\frac{\theta}{2} - e^{2i\phi}\sinh^2\frac{\theta}{2})$$
$$- \omega\sin\varphi(\cosh^2\frac{\theta}{2} + e^{2i\phi}\sinh^2\frac{\theta}{2})] + \frac{\Omega}{2}e^{i\phi}\sinh\theta,$$

and

$$C = \frac{\sqrt{2}G\gamma}{\sqrt{N}}[i\Omega\cos\varphi(\cosh^2\frac{\theta}{2} - e^{-2i\phi}\sinh^2\frac{\theta}{2})$$
$$+ \omega\sin\varphi(\cosh^2\frac{\theta}{2} + e^{-2i\phi}\sinh^2\frac{\theta}{2})] - \frac{\Omega}{2}e^{-i\phi}\sinh\theta.$$

The Hermitian Hamiltonian can be indeed obtained under the condition $B = C = 0$, from which the pending parameters is determined as

$$\cos\phi = \frac{\eta\sin\varphi}{\sqrt{\Phi(\eta,\varphi)}},$$

and

$$\cosh\theta = \pm\frac{1}{\sqrt{1 - 2^3G^2\frac{\gamma^2}{N}\Phi(\eta,\varphi)}}.$$

We obtain

$$A = \Omega\sqrt{1 - 2^3G^2\frac{\gamma^2}{N}\Phi(\eta,\varphi)}. \tag{54}$$

The Hamiltonian after transformation

$$\widehat{h} = \omega\gamma^2 + A\widehat{S}_z, \tag{55}$$

is Hermitian under condition

$$2^3G^2\frac{\gamma^2}{N}\Phi(\eta,\varphi) \leq 1.$$

The Hamiltonian Eq. (55) has eigenstates $\widehat{h}|\pm s\rangle = \pm s|\pm s\rangle$ with $s = N$ being the extremum SCSs. The eigenstates of original non-Hermitian Hamiltonians are seen to be form Eq. (52)

$$\widehat{H}_{eff}|\pm u\rangle_r = E_\pm|\pm u\rangle_r,$$
$$\widehat{H}^\dagger_{eff}|\pm u\rangle_l = E_\pm|\pm u\rangle_l,$$

in which

$$|\pm u\rangle_r = \widehat{R}^{-1}|\pm s\rangle,$$
$$|\pm u\rangle_l = \widehat{R}|\pm s\rangle,$$

are called respectively the "ket" and "bra" states related by a metric operator

$$\widehat{\chi} = \widehat{R}^2$$

such that

$$|\pm u\rangle_l = \widehat{\chi}|\pm u\rangle_r.$$

The semiclassical energy functions are obtained as

$$E_\pm(\gamma) = {}_l\langle\pm u|\widehat{H}_{eff}|\pm u\rangle_r = N\varepsilon_\pm(\gamma), \tag{56}$$

with

$$\varepsilon_\pm(\gamma) = \omega\frac{\gamma^2}{N} \pm A. \tag{57}$$

### A. Exceptional point of semiclassical energy function

An important observation for the non-Hermitian Hamiltonian is that the energy functions Eq. (56) are not always real. An exceptional point (EP)

$$G_{ep} = \frac{\sqrt{N}}{2\sqrt{2}\gamma}\frac{1}{\sqrt{\Phi(\eta,\varphi)}}, \tag{58}$$

exists. The energy function is real below $G_{ep}$, while becomes complex when $G > G_{ep}$.

The variations of real part (1) and imaginary part (2) of energy functions $\varepsilon_\pm(\gamma)$ Eq. (56) with respect to the atom-field coupling $G$ are displayed in Fig. 7 under the resonance $\eta = 1$ with given cavity-field parameter $\gamma^2/N = 1$ (a), 2 (b). Two branches of the energy function $\varepsilon_\pm(\gamma)$ are represented respectively by the red and black solid lines. In the region $G < G_{ep}$, the real part of energy functions have two branches, while the imaginary
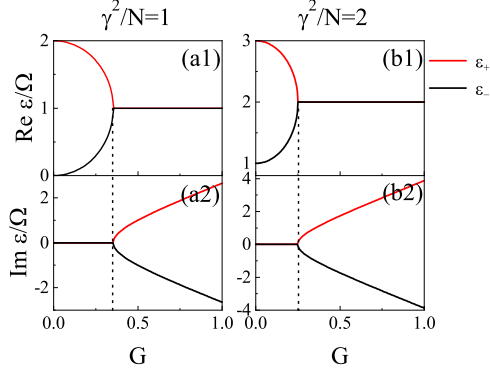
FIG. 7: Real (1) and imaginary (2) parts of energy functions $\varepsilon_\pm(\gamma)$ as a function of the dimensionless atom-field coupling strength $G$ for the parameter $\gamma^2/N = 1$ (a), 2 (b) with $\eta = 1$, $\varphi = \pi/3$.

part is zero. However, the situation is just opposite for $G > G_{ep}$.

Fig. 8 shows the variations of energy functions $\varepsilon_\pm(\gamma)$ with respect to the cavity-field parameter $\gamma^2/N$ under the resonance ($\eta = 1$).
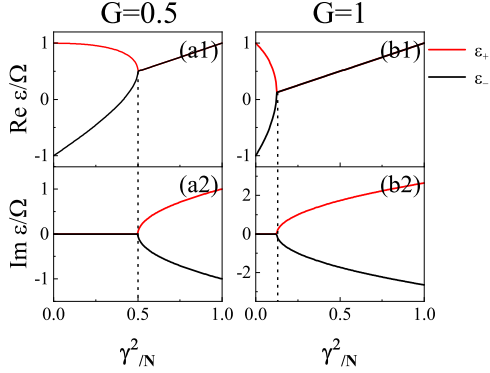


FIG. 8: The variations of real (1) and imaginary (2) parts of energy functions $\varepsilon_\pm(\gamma)$ with respect to the cavity-field parameter $\gamma^2/N$ for the atom-field coupling strength $G = 0.5$ (a), 1 (b) with $\eta = 1$, $\varphi = \pi/3$.

### B. Variational ground state

We now investigate the variational ground state with the energy function given by Eq. (57)

$$\varepsilon_\pm(\gamma) = \frac{\omega\gamma^2}{N} \pm \Omega\sqrt{1 - \frac{2^3 G^2 \gamma^2}{N}\Phi(\eta,\varphi)}.$$

By the variation with respect to parameter $\gamma$, we find that the spin down state $\varepsilon_-(\gamma = 0)$ of zero photon is stable in the whole region of $G$ different from the Hermitian case where the NP exists only in lower value region.

While the stable spin-up state $\varepsilon_+(\gamma = 0)$ is valid only when $G \leq G_c$ with

$$G_c = \frac{1}{2}\sqrt{\frac{\eta}{\Phi(\eta,\varphi)}}. \tag{59}$$

The extremum equation

$$\frac{\partial \varepsilon_\pm(\gamma)}{\partial\gamma} = 0,$$

does not have a non-zero solution for spin down state $\varepsilon_-$. The non-zero solution for the spin-up state $\varepsilon_+$ is found as

$$n_p = \frac{\gamma_c^2}{N} = \frac{1 - \frac{2^4}{\eta^2}G^4\Phi^2(\eta,\varphi)}{2^3 G^2 \Phi(\eta,\varphi)} \tag{60}$$

under the condition $G \leq G_c$. However the non-zero solution $\varepsilon_+(\gamma_c)$ is unstable since the second-order derivative is negative $\frac{\partial^2 \varepsilon_+}{\partial\gamma^2}(\gamma_c) < 0$. The average energy of unstable state $\varepsilon_+(\gamma_c)$ is given by

$$\varepsilon_+(n_p) = \omega n_p + \Omega\sqrt{1 - 2^3 G^2 n_p \Phi(\eta,\varphi)}, \tag{61}$$

which is real for the valid photon number $n_p \geq 0$ in Eq. (60). Thus the complex energies and EP are excluded in the ground state. Fig. 9 displays the energy spectrum, photon number and atom energy $\varepsilon_a = \varepsilon_+ - \omega n_p$ for the unstable state $\widetilde{S}_+$.
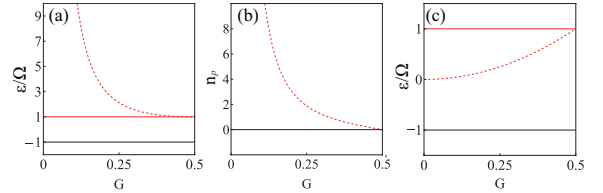


FIG. 9: Average energy $\varepsilon$ (a) photon number $n_p$ (b) and atom energy $\varepsilon_a$ (c) as functions of the coupling strength $G$ in the resonance $\eta = 1$, at field phase angle $\varphi = \pi/3$. $\widetilde{S}_+$ (red dash curve) denotes the unstable superradiant state. $N_\pm$ (red, black solid curves) denote the normal states.

Fig. 10 is the $G - \eta$ phase diagram in unified gauge, where the photon number of state $\widetilde{S}_+$ is measured in color scale. $NP(N_-)$ denoting the NP with the normal state $N_-$ (dark blue region) is located on the right of phase boundary $G_c$. $NP_{co}(N_-, N_+, \widetilde{S}_+)$ means the $NP(N_-)$ coexisting with higher energy states $N_+, \widetilde{S}_+$. The SP does not exists since superradiant state $\widetilde{S}_+$ is unstable due to the photon number loss induced by the non-Hermitian interaction. The QPT does not appear either.
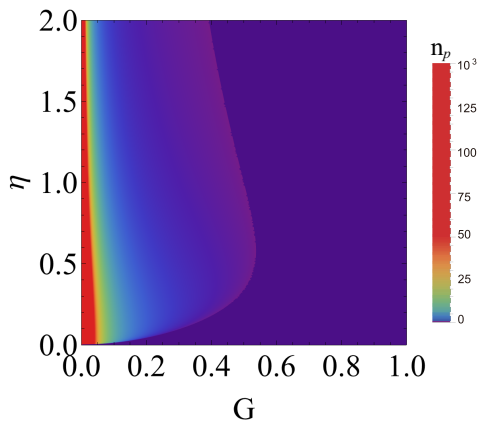
FIG. 10: $G - \eta$ phase diagram in the unified gauge with the field phase angle $\varphi = \pi/3$.

## VI. CONCLUSION

We clarify in this article the gauge equivalence for the atom field interaction. Since the Hamiltonian is explicitly time dependent with the time varying field, the gauge transformation has to be applied on the time-dependent Schrődinger equation. Not only the transformed Hamiltonian but also the basis vectors should be taken into account in the new gauge. Thus the Hamiltonian called unified gauge is truly gauge equivalent to the minimum coupling principle Eq. (1). The Hamiltonians of three gauges are compared with the system of three-level atom in an optical cavity. The Hamiltonian of unified gauge includes both interactions of Coulomb and dipole gauges.

We solve the DM Hamiltonians of $\Xi$-type three-level atoms in terms of SCS variational method, where the three-level atom is described by pseudospin operators of spin-1. The variational ground state of unified gauge depends on the photon number as well as general phase-angle of cavity field. The results of Coulomb and dipole gauges are just the special cases of the unified gauge. A remarkable observation is that the ground states of three gauges coincide exactly in the resonance condition $\eta = 1$. The QPT is analyzed explicitly as a comparison of three gauges. We reveal a phase-sensitive effect in the unified gauge for the three-level system, where photon-number distributions depend critically on the initial phase of the optical field. This constitutes a crucial feature widely overlooked in the two-level atom DM with the usual Coulomb gauge interaction [39, 45, 75, 81].

The coupling constant between cavity-field and atom is proportional to the dipole matrix elements $\mathbf{x}_{ij}$, which are known as complex values. The non-Hermitian Hamiltonian is obtained naturally by choosing the real part of dipole matrix element. The semiclassical energy function averaged in the trial wave function is indeed not always real. It becomes complex beyond the EP $G_{ep}$. However the variational ground-state energy remains real excluding the complex value as well as the EP. The superradiant state becomes unstable because of photon number loss induced by the non-Hermitian interaction. Thus the QPT does not exist in the non-Hermitian DM Hamiltonian.

[1] I. J. R. Aitchison and A. J. G. Hey. *Gauge Theories in Particle Physics*. Adam Hilger, 1989.

[2] Gian Marcello Andolina, Paolo Andrea Erdman, Frank Noé, Jukka Pekola, and Marco Schirò. Dicke superradiant heat current enhancement in circuit quantum electrodynamics. *Phys. Rev. Res.*, 6:043128, Nov 2024.

[3] Frank Arute, Kunal Arya, Ryan Babbush, Dave Bacon, Joseph C. Bardin, Rami Barends, Rupak Biswas, Sergio Boixo, Fernando G. S. L. Brandao, David A. Buell, Brian Burkett, Yu Chen, Zijun Chen, Ben Chiaro, Roberto Collins, William Courtney, Andrew Dunsworth, Edward Farhi, Brooks Foxen, Austin Fowler, Craig Gidney, Marissa Giustina, Rob Graff, Keith Guerin, Steve Habegger, Matthew P. Harrigan, Michael J. Hartmann, Alan Ho, Markus Hoffmann, Trent Huang, Travis S. Humble, Sergei V. Isakov, Evan Jeffrey, Zhang Jiang, Dvir Kafri, Kostyantyn Kechedzhi, Julian Kelly, Paul V. Klimov, Sergey Knysh, Alexander Korotkov, Fedor Kostritsa, David Landhuis, Mike Lindmark, Erik Lucero, Dmitry Lyakh, Salvatore Mandrà, Jarrod R. McClean, Matthew McEwen, Anthony Megrant, Xiao Mi, Kristel Michielsen, Masoud Mohseni, Josh Mutus, Ofer Naaman, Matthew Neeley, Charles Neill, Murphy Yuezhen Niu, Eric Ostby, Andre Petukhov, John C. Platt, Chris Quintana, Eleanor G. Rieffel, Pedram Roushan, Nicholas C. Rubin, Daniel Sank, Kevin J. Satzinger, Vadim Smelyanskiy, Kevin J. Sung, Matthew D. Trevithick, Amit Vainsencher, Benjamin Villalonga, Theodore White, Z. Jamie Yao, Ping Yeh, Adam Zalcman, Hartmut Neven, and John M. Martinis. Quantum supremacy using a programmable superconducting processor. *Nature*, 574(7779):505–510, Oct 2019.

[4] M. Babiker and Rodney Loudon. Derivation of the power-zienau-woolley hamiltonian in quantum electrodynamics by gauge transformation. *Proc. R. Soc. Lond. A*, 385(1789):439–460, 1983.

[5] Alexandre Baksic, Pierre Nataf, and Cristiano Ciuti. Superradiant phase transitions with three-level systems.

*Phys. Rev. A*, 87:023813, Feb 2013.

[6] F. Bassani, J. J. Forney, and A. Quattropani. Choice of gauge in two-photon transitions: $1s - 2s$ transition in atomic hydrogen. *Phys. Rev. Lett.*, 39:1070–1073, Oct 1977.

[7] Kristian Baumann, Christine Guerlin, Ferdinand Brennecke, and Tilman Esslinger. Dicke quantum phase transition with a superfluid gas in an optical cavity. *Nature*, 464(7293):1301–1306, Apr 2010.

[8] Justin G. Bohnet, Zilong Chen, Joshua M. Weiner, Dominic Meiser, Murray J. Holland, and James K. Thompson. A steady-state superradiant laser with less than one intracavity photon. *Nature*, 484(7392):78–81, Apr 2012.

[9] K.-J. Boller, A. Imamoğlu, and S. E. Harris. Observation of electromagnetically induced transparency. *Phys. Rev. Lett.*, 66:2593–2596, May 1991.

[10] Gang Chen, Juqi Li, and J.-Q. Liang. Critical property of the geometric phase in the dicke model. *Phys. Rev. A*, 74:054101, Nov 2006.

[11] Yu-Yuan Chen, Jian-Jian Cheng, Chong Ye, and Yong Li. Enantiodetection of cyclic three-level chiral molecules in a driven cavity. *Phys. Rev. Res.*, 4:013100, Feb 2022.

[12] Ezequiel I. Rodríguez Chiacchio, Andreas Nunnenkamp, and Matteo Brunelli. Nonreciprocal dicke model. *Phys. Rev. Lett.*, 131:113602, Sep 2023.

[13] M. M. Cola, D. Bigerni, and N. Piovella. Recoil-induced subradiance in an ultracold atomic gas. *Phys. Rev. A*, 79:053622, May 2009.

[14] S. Cordero, R. López-Peña, O. Castaños, and E. Nahmad-Achar. Quantum phase transitions of three-level atoms interacting with a one-mode electromagnetic field. *Phys. Rev. A*, 87:023805, Feb 2013.

[15] A. Crubellier, S. Liberman, D. Pavolini, and P. Pillet. Superradiance and subradiance. i. interatomic interference and symmetry properties in three-level systems. *J. Phys. B: At. Mol. Phys.*, 18(18):3811, sep 1985.

[16] A. Crubellier and D. Pavolini. Superradiance and subradiance. ii. atomic systems with degenerate transitions. *J. Phys. B: At. Mol. Phys.*, 19(14):2109, jul 1986.

[17] Daniele De Bernardis, Tuomas Jaako, and Peter Rabl. Cavity quantum electrodynamics in the nonperturbative regime. *Phys. Rev. A*, 97:043820, Apr 2018.

[18] Daniele De Bernardis, Philipp Pilar, Tuomas Jaako, Simone De Liberato, and Peter Rabl. Breakdown of gauge invariance in ultrastrong-coupling cavity qed. *Phys. Rev. A*, 98:053819, Nov 2018.

[19] Omar Di Stefano, Alessio Settineri, Vincenzo Macrì, Luigi Garziano, Roberto Stassi, Salvatore Savasta, and Franco Nori. Resolution of gauge ambiguities in ultrastrong-coupling cavity quantum electrodynamics. *Nat. Phys.*, 15(8):803–808, aug 2019.

[20] R. H. Dicke. Coherence in spontaneous radiation processes. *Phys. Rev.*, 93:99–110, Jan 1954.

[21] Wenkui Ding, Xiaoguang Wang, and Shu Chen. Fundamental sensitivity limits for non-hermitian quantum sensors. *Phys. Rev. Lett.*, 131:160801, Oct 2023.

[22] Fu-Quan Dou, Yuan-Jin Wang, and Jian-An Sun. Closed-loop three-level charged quantum battery. *Europhys. Lett.*, 131(4):43001, sep 2020.

[23] Fu-Quan Dou, Yuan-Jin Wang, and Jian-An Sun. Highly efficient charging and discharging of three-level quantum batteries through shortcuts to adiabaticity. *Front. Phys.*, 17(3):31503, Nov 2021.

[24] Ramy El-Ganainy, Mercedeh Khajavikhan, Demetrios N. Christodoulides, and Sahin K. Ozdemir. The dawn of non-hermitian optics. *Commun. Phys.*, 2(1):37, mar 2019.

[25] Diego Fallas Padilla and Han Pu. Tricritical dicke model with and without dissipation. *Phys. Rev. A*, 108:033706, Sep 2023.

[26] Jingtao Fan and Suotang Jia. Collective dynamics of the unbalanced three-level dicke model. *Phys. Rev. A*, 107:033711, Mar 2023.

[27] Michael Fleischhauer, Atac Imamoglu, and Jonathan P. Marangos. Electromagnetically induced transparency: Optics in coherent media. *Rev. Mod. Phys.*, 77:633–673, Jul 2005.

[28] Anton Frisk Kockum, Adam Miranowicz, Simone De Liberato, Salvatore Savasta, and Franco Nori. Ultrastrong coupling between light and matter. *Nat. Rev. Phys.*, 1(1):19–40, Jan 2019.

[29] R. Girlanda, A. Quattropani, and P. Schwendimann. Two-photon transitions to exciton states in semiconductors. application to cucl. *Phys. Rev. B*, 24:2009–2017, Aug 1981.

[30] M. Gross, C. Fabre, P. Pillet, and S. Haroche. Observation of near-infrared dicke superradiance on cascading transitions in atomic sodium. *Phys. Rev. Lett.*, 36:1035–1038, Apr 1976.

[31] Mathias Hayn, Clive Emary, and Tobias Brandes. Phase transitions and dark-state physics in two-color superradiance. *Phys. Rev. A*, 84:053856, Nov 2011.

[32] Mathias Hayn, Clive Emary, and Tobias Brandes. Superradiant phase transition in a model of three-level-$\Lambda$ systems interacting with two bosonic modes. *Phys. Rev. A*, 86:063822, Dec 2012.

[33] Sohrab Ismail-Beigi, Eric K. Chang, and Steven G. Louie. Coupling of nonlocal potentials to electromagnetic fields. *Phys. Rev. Lett.*, 87:087402, Aug 2001.

[34] Dasom Kim, Sohail Dasgupta, Xiaoxuan Ma, Joong-Mok Park, Hao-Tian Wei, Xinwei Li, Liang Luo, Jacques Doumani, Wanting Yang, Di Cheng, Richard H. J. Kim, Henry O. Everitt, Shojiro Kimura, Hiroyuki Nojiri, Jigang Wang, Shixun Cao, Motoaki Bamba, Kaden R. A. Hazzard, and Junichiro Kono. Observation of the magnonic dicke superradiant phase transition. *Sci. Adv.*, 11(14):eadt1691, 2025.

[35] Phatthamon Kongkhambut, Hans Keßler, Jim Skulte, Ludwig Mathey, Jayson G. Cosme, and Andreas Hemmerich. Realization of a periodically driven open three-level dicke model. *Phys. Rev. Lett.*, 127:253601, Dec 2021.

[36] Willis E. Lamb. Fine structure of the hydrogen atom. iii. *Phys. Rev.*, 85:259–276, Jan 1952.

[37] Willis E. Lamb, Rainer R. Schlicher, and Marlan O. Scully. Matter-field interaction in atomic physics and quantum optics. *Phys. Rev. A*, 36:2763–2772, Sep 1987.

[38] C. Leonardi, F. Persico, and G. Vetri. Dicke model and the theory of driven and spontaneous emission. *Riv. Nuovo Cim.*, 9(4):1–85, apr 1986.

[39] Jin-Ling Lian, Yuan-Wei Zhang, and Jiu-Qing Liang. Macroscopic quantum states and quantum phase transition in the dicke model. *Chin. Phys. Lett.*, 29(6):060302, jun 2012.

[40] J.-Q. Liang and L. F. Wei. *New Advances in Quantum Physics.* Science Press, Beijing, third edition, 2023.

[41] Ni Liu, Shan Huang, and J.-Q. Liang. Macroscopic quantum states in dicke model of pt-symmetric non-hermitian

hamiltonian and superradiant phase with imaginary atomic population. *Results Phys.*, 40:105813, 2022.

[42] Peter Lodahl, Sahand Mahmoodian, Søren Stobbe, Arno Rauschenbeutel, Philipp Schneeweiss, Jürgen Volz, Hannes Pichler, and Peter Zoller. Chiral quantum optics. *Nature*, 541(7638):473–480, jan 2017.

[43] Rodney Loudon. *The quantum theory of light.* OUP Oxford, 2000.

[44] Xilin Lu, Hui Li, Jia-Kai Shi, Li-Bao Fan, Vladimir Mangazeev, Zi-Min Li, and Murray T. Batchelor. $\mathcal{PT}$-symmetric quantum rabi model. *Phys. Rev. A*, 108:053712, Nov 2023.

[45] Yunqing Luo, Ni Liu, and J.-Q. Liang. Quantum phase transition and exceptional points of a non-hermitian hamiltonian for cold atoms in a dissipative optical cavity with nonlinear atom-photon interactions. *Phys. Rev. A*, 110:063320, Dec 2024.

[46] Lars S. Madsen, Fabian Laudenbach, Mohsen Falamarzi. Askarani, Fabien Rortais, Trevor Vincent, Jacob F. F. Bulmer, Filippo M. Miatto, Leonhard Neuhaus, Lukas G. Helt, Matthew J. Collins, Adriana E. Lita, Thomas Gerrits, Sae Woo Nam, Varun D. Vaidya, Matteo Menotti, Ish Dhand, Zachary Vernon, Nicolás Quesada, and Jonathan Lavoie. Quantum computational advantage with a programmable photonic processor. *Nature*, 606(7912):75–81, Jun 2022.

[47] Michele Maggiore. *A modern introduction to quantum field theory*, volume 12. Oxford university press, 2005.

[48] Haiyu Meng, Yee Sin Ang, and Ching Hua Lee. Exceptional points in non-hermitian systems: Applications and recent developments. *Appl. Phys. Lett.*, 124(6):060502, feb 2024.

[49] Peter W Milonni. *An introduction to quantum optics and quantum fluctuations.* Oxford University Press, 2019.

[50] J Mompart and R Corbalán. Lasing without inversion. *J. Opt. B: Quantum Semiclass. Opt.*, 2(3):R7, jun 2000.

[51] Ali Mostafazadeh. Pseudo-hermiticity versus pt symmetry: The necessary condition for the reality of the spectrum of a non-hermitian hamiltonian. *J. Math. Phys.*, 43(1):205–214, jan 2002.

[52] Ali Mostafazadeh. Pseudo-supersymmetric quantum mechanics and isospectral pseudo-hermitian hamiltonians. *Nucl. Phys. B*, 640(3):419–434, 2002.

[53] Ali Mostafazadeh. Time-dependent pseudo-hermitian hamiltonians defining a unitary quantum system and uniqueness of the metric operator. *Phys. Lett. B*, 650(2):208–212, 2007.

[54] T. Niemczyk, F. Deppe, H. Huebl, E. P. Menzel, F. Hocke, M. J. Schwarz, J. J. Garcia-Ripoll, D. Zueco, T. Hümmer, E. Solano, A. Marx, and R. Gross. Circuit quantum electrodynamics in the ultrastrong-coupling regime. *Nat. Phys.*, 6(10):772–776, Oct 2010.

[55] Jin-Sheng Peng and Gao-Xiang Li. *Introduction to modern quantum optics.* World Scientific, 1998.

[56] Alexander N. Poddubny, Serge Rosenblum, and Barak Dayan. How single-photon switching is quenched with multiple Λ–level atoms. *Phys. Rev. Lett.*, 133:113601, Sep 2024.

[57] Aneesh Ramaswamy and Svetlana A. Malinovskaya. Entanglement transfer of a rydberg w-state to a multi-mode photonic state. *Phys. Rev. Res.*, 7:013288, Mar 2025.

[58] K. Rzążewski and R. W. Boyd. Equivalence of interaction hamiltonians in the electric dipole approximation. *J. Mod. Opt.*, 51(8):1137–1147, may 2004.

[59] S. Samimi and M. M. Golshan. Characteristics of superradiant optical phases occurring in the system of nondegenerate Λ atoms and radiation that are interacting inside a nonlinear quantum cavity. *Phys. Rev. A*, 105:053702, May 2022.

[60] Alan C. Santos, Andreia Saguia, and Marcelo S. Sarandy. Stable and charge-switchable quantum batteries. *Phys. Rev. E*, 101:062114, Jun 2020.

[61] Michael Scheibner, Thomas Schmidt, Lukas Worschech, Alfred Forchel, Gerd Bacher, Thorsten Passow, and Detlef Hommel. Superradiance of quantum dots. *Nat. Phys.*, 3(2):106–110, Feb 2007.

[62] Marlan O. Scully, Shi-Yao Zhu, and Athanasios Gavrielides. Degenerate quantum-beat laser: Lasing without inversion and inversion without lasing. *Phys. Rev. Lett.*, 62:2813–2816, Jun 1989.

[63] N. Skribanowitz, I. P. Herman, J. C. MacGillivray, and M. S. Feld. Observation of dicke superradiance in optically pumped hf gas. *Phys. Rev. Lett.*, 30:309–312, Feb 1973.

[64] Jim Skulte, Phatthamon Kongkhambut, Hans Keßler, Andreas Hemmerich, Ludwig Mathey, and Jayson G. Cosme. Parametrically driven dissipative three-level dicke model. *Phys. Rev. A*, 104:063705, Dec 2021.

[65] Anthony F. Starace. Length and velocity formulas in approximate oscillator-strength calculations. *Phys. Rev. A*, 3:1242–1245, Apr 1971.

[66] Roberto Stassi, Mauro Cirio, and Franco Nori. Scalable quantum computer with superconducting circuits in the ultrastrong coupling regime. *npj Quantum Inf.*, 6(1):67, Aug 2020.

[67] Adam Stokes and Ahsan Nazir. Gauge ambiguities imply jaynes-cummings physics remains valid in ultrastrong coupling qed. *Nat. Commun.*, 10(1):499, jan 2019.

[68] Adam Stokes and Ahsan Nazir. Gauge non-invariance due to material truncation in ultrastrong-coupling quantum electrodynamics. *Nat. Phys.*, 20(3):376–378, mar 2024.

[69] Yue Sun, Tao Shi, Zhiyong Liu, Zhidong Zhang, Liantuan Xiao, Suotang Jia, and Ying Hu. Fractional quantum zeno effect emerging from non-hermitian physics. *Phys. Rev. X*, 13:031009, Jul 2023.

[70] C. C. Sung and C. M. Bowden. Phase transition in the multimode two- and three-level dicke model (green's function method). *J. Phys. A: Math. Gen.*, 12(11):2273, nov 1979.

[71] Michael A. D. Taylor, Arkajit Mandal, Wanghuai Zhou, and Pengfei Huo. Resolution of gauge ambiguities in molecular cavity quantum electrodynamics. *Phys. Rev. Lett.*, 125:123602, Sep 2020.

[72] Changqing Wang, Zhoutian Fu, Wenbo Mao, Jinran Qie, A Douglas Stone, and Lan Yang. Non-hermitian optics and photonics: from classical to quantum. *Adv. Opt. Photon.*, 15(2):442–523, 2023.

[73] Shuai-Peng Wang, Guo-Qiang Zhang, Yimin Wang, Zhen Chen, Tiefu Li, J. S. Tsai, Shi-Yao Zhu, and J. Q. You. Photon-dressed bloch-siegert shift in an ultrastrongly coupled circuit quantum electrodynamical system. *Phys. Rev. Appl.*, 13:054063, May 2020.

[74] Yi-Cheng Wang, Jhih-Shih You, and H. H. Jen. A non-hermitian optical atomic mirror. *Nat. Commun.*, 13(1):4598, aug 2022.

[75] Zhimei Wang, Jinling Lian, J.-Q. Liang, Yanmei Yu, and Wu-Ming Liu. Collapse of the superradiant phase and

multiple quantum phase transitions for bose-einstein condensates in an optomechanical cavity. *Phys. Rev. A*, 93:033630, Mar 2016.

[76] Frank Wilczek. In search of symmetry lost. *Nature*, 433(7023):239–247, Jan 2005.

[77] Frank Wilczek. Minimalism triumphant. *Nature*, 496(7446):439–441, Apr 2013.

[78] P. Wolf, S. C. Schuster, D. Schmidt, S. Slama, and C. Zimmermann. Observation of subradiant atomic momentum states with bose-einstein condensates in a recoil resolving optical ring resonator. *Phys. Rev. Lett.*, 121:173602, Oct 2018.

[79] Fumiki Yoshihara, Tomoko Fuse, Sahel Ashhab, Kosuke Kakuyanagi, Shiro Saito, and Kouichi Semba. Superconducting qubit–oscillator circuit beyond the ultrastrong-coupling regime. *Nat. Phys.*, 13(1):44–47, Jan 2017.

[80] Guo-Qiang Zhang, Zhen Chen, and J. Q. You. Experimentally accessible quantum phase transition in a non-hermitian tavis-cummings model engineered with two drive fields. *Phys. Rev. A*, 102:032202, Sep 2020.

[81] Xiuqin Zhao, Ni Liu, and J.-Q. Liang. Nonlinear atom-photon-interaction-induced population inversion and in-verted quantum phase transition of bose-einstein condensate in an optical cavity. *Phys. Rev. A*, 90:023622, Aug 2014.

[82] Han-Sen Zhong, Yu-Hao Deng, Jian Qin, Hui Wang, Ming-Cheng Chen, Li-Chao Peng, Yi-Han Luo, Dian Wu, Si-Qiu Gong, Hao Su, Yi Hu, Peng Hu, Xiao-Yan Yang, Wei-Jun Zhang, Hao Li, Yuxuan Li, Xiao Jiang, Lin Gan, Guangwen Yang, Lixing You, Zhen Wang, Li Li, Nai-Le Liu, Jelmer J. Renema, Chao-Yang Lu, and Jian-Wei Pan. Phase-programmable gaussian boson sampling using stimulated squeezed light. *Phys. Rev. Lett.*, 127:180502, Oct 2021.

[83] Han-Sen Zhong, Hui Wang, Yu-Hao Deng, Ming-Cheng Chen, Li-Chao Peng, Yi-Han Luo, Jian Qin, Dian Wu, Xing Ding, Yi Hu, Peng Hu, Xiao-Yan Yang, Wei-Jun Zhang, Hao Li, Yuxuan Li, Xiao Jiang, Lin Gan, Guangwen Yang, Lixing You, Zhen Wang, Li Li, Nai-Le Liu, Chao-Yang Lu, and Jian-Wei Pan. Quantum computational advantage using photons. *Science*, 370(6523):1460–1463, 2020.